Journal of Petroleum Science and Engineering 201 (2021) 108500

Contents lists available at ScienceDirect

Journal of Petroleum Science and Engineering

journal homepage: http://www.elsevier.com/locate/petrol

A Single Well Chemical Tracer model that accounts for temperature gradients, pH changes and buffering

Tom Pedersen

Department of Tracer Technology, Institute for Energy Technology, P.OB. ox 40, Kjeller, 2027, Norway

ARTICLE INFO

Keywords:
SWCT
Residual oil saturation
Tracers
Temperature gradients
pH changes
Numerical model

ABSTRACT

We present the first ever Single Well Chemical Tracer (SWCT) model that incorporates temperature gradients and pH-driven ethyl acetate hydrolysis rate changes when buffering by either calcite in the oil-bearing formation or by chemical species in the injected brine are accounted for. The model is applied to four generic cases with SWCT test, rock formation and brine composition data based on published values. An analytical model is used to calculate how the brine injection temperature decreases with time and an axially symmetric numerical model is used to simulate the cooling of the oil-bearing formation, chemical reactions and transport of species in the reservoir. The primary oil-water partitioning tracer ethyl acetate hydrolyses into the secondary water tracer ethanol and acetic acid that lowers the pH and changes the hydrolysis rate. The acid driven pH decrease may be significantly reduced by pH buffering mechanisms. We investigate four different buffer models. Model 1 may represent a sandstone with calcite cement. In Model 2, also with calcite cement, the brine has less calcium but more bicarbonate and initially lower pH than Model 1. Model 3 is a clean sandstone without calcite cement and the brine contains no calcium but much bicarbonate. Model 4 has no buffer capacity neither in the brine nor in the target formation. Although we discuss only four models, they are quite different and represent an important subset of the realistic SWCT test parameter space. A temperature gradient develops across the primary tracer bank in all four models and this causes the secondary tracer to be displaced away from the wellbore relative to the primary tracer. We find that most of the ethyl acetate hydrolysis takes place during shut-in. The residual oil saturation (S_{or}) is estimated from the synthetic tracer production curves using the simple chromatographic separation equation as well as with the mean residence time correction. The two methods underestimate the true S_{or} value (22%) by 3–5 and 3–11% (saturation points), respectively. These results demonstrate that the 'handicap' created by the temperature gradient together with the pH-driven hydrolysis rate changes should be taken into account in S_{or} estimates. We suggest that SWCT tests may be used to evaluate the effective wettability of the target formation at a modest extra cost. Using water tracers with very low quantification limits as primary tracers should reduce or even eliminate the problems caused by temperature gradients and pH-driven hydrolysis rate changes since they will travel well ahead of the temperature gradient and the small amount of acid generated will produce only an insignificant reduction in pH.

1. Introduction

Single Well Chemical Tracer (SWCT) tests are performed in oil producers to estimate the residual oil saturation (S_{or}), i.e., the fraction of pore volume occupied by immobile oil after a displacement process. S_{or} is a function of initial saturation, lithology, petrophysical properties, fluid characteristics, recovery methods and production history (Teklu et al., 2013). Reliable estimates of S_{or} are important for reserve assessment, recovery calculations and for increasing our understanding of oil field behavior. One of the most important applications of SWCT tests is to gauge the performance of Enhanced Oil Recovery (EOR) methods. The reduction in S_{or} between SWCT tests conducted before and after an EOR operation has been used to measure the efficiency of hydrocarbon miscible gas floods (Cockin et al., 2000), low salinity water floods (Skrettingland et al., 2010; Khaledialidusti et al., 2015; Al-Shalabi et al., 2017; Kazemi et al., 2019), alkaline-surfactant-polymer (ASP) floods (Carlisle et al., 2014; Fortenberry et al., 2016) just to mention some examples. We estimate that close to a thousand SWCT tests have been

E-mail address: Tom.Pedersen@ife.no.
URL: http://www.ife.no.

https://doi.org/10.1016/j.petrol.2021.108500
Received 21 December 2020; Accepted 1 February 2021
Available online 9 February 2021

executed worldwide in all types of reservoirs during the last fifty years. The use of SWCT tests appears to increase annually.

The fundamental mechanism utilized in the SWCT method is the chromatographic separation between an oil-water partitioning tracer and a water tracer when they move towards the producer from a distance of a few meters. Since oil-water partitioning tracers spend some time in the immobile oil, they move more slowly than water tracers that move with the flowing water all the time. The velocity difference depends on S_{or} and the distribution constant (partitioning coefficient), i.e., the ratio of the oil-water tracer concentration in oil to its concentration in water. The distribution constant can be measured in the laboratory. Together with tracer information gathered by the SWCT test, it is possible to estimate S_{or}. Based on work performed by Exxon Research in East Texas in the late 60's, Deans (1971) patented the seminal idea to use the oil-water partitioning (primary) tracer itself to generate the (secondary) water tracer *in-situ* by hydrolysis, i.e., the primary tracer is reactive as well as partitioning.

A prerequisite for the SWCT method to work is that the oil in the target formation is at residual oil saturation. A 98% or higher water-cut is often considered a practical criterion for the oil to be virtually immobile (Deans and Majoros, 1980). If the well has a significant oil-cut, a local water flood is performed before the SWCT test in order to reduce the oil saturation to residual (e.g., Carlisle et al., 2014). The SWCT test proper starts by pumping the primary tracer dissolved in brine from the producer into the oil-bearing target formation where S_{or} is to be measured (Fig. 1).

The primary tracer is followed by a slug of tracer free brine. The depth of investigation into the oil-bearing formation (typically a few meters) can be controlled by varying the pump rate and duration of the tracer and brine injections. The primary partitioning tracer is subsequently left to partly hydrolyze into the secondary water tracer. Deans and Majoros (1980) recommended that the shut-in should last sufficiently long for at least 50% of the hydrolysis to take place during shut-in, i.e., when the tracers are stagnant, since a basic assumption in utilizing the chromatographic separation to calculate S_{or} is that the oil-water and water tracers both start towards the wellbore from the same position, i.e., distance from the wellbore. After shut-in, the tracers are back produced, and their concentrations monitored as functions of produced volume or time. In some cases, S_{or} can be calculated analytically from the oil-water and water tracer curves like in inter-well tracer tests (Cook, 1971). The inevitable dispersion that occurs when the tracers move through the permeable rock can to some degree be accounted for by using the mean residence times in Cook's (1971) chromatography formula (Deans and Majoros, 1980; Shook et al., 2009). Doorwar et al. (2020) present an analytical method that in addition to the distribution constant also considers shut-in duration and an 'average hydrolyses rate'. In most cases, however, computer simulations are required to obtain a good S_{or} estimate (Deans and Majoros, 1980; Deans and Carlisle, 1986; Jerauld et al., 2010; Mechergui et al., 2012; Kazemi et al., 2019). Deans and Majoros (1980) give a thorough review of the SWCT method and present detailed results from 59 tests. Deans and Carlisle (2007) present an updated discussion of the method and its applications. Khaledialidusti et al. (2014) discuss several unconventional (non-chemical) single well models. To the best of our knowledge, none of these have been tested in the field.

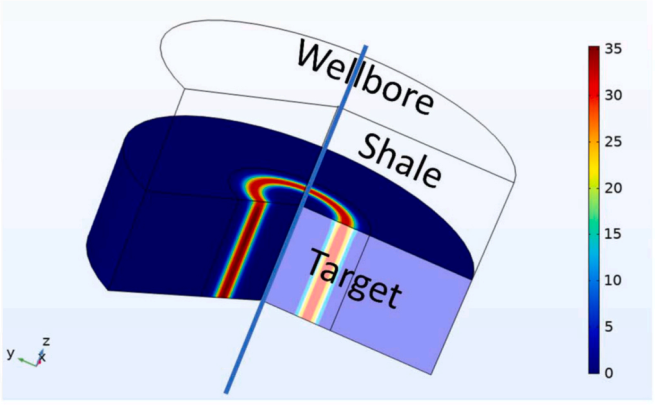

Fig. 1. The axially symmetric SWCT model configuration used in this paper (i.e., the model appears unchanged if rotated around the wellbore). The permeable target formation ('Target') is found between impermeable shales ('Shale'; only upper layers shown). Assuming an axially symmetric model makes it possible to obtain a full 3D solution by solving the differential equations for temperature and chemical species in the 2D plane labeled 'Target' only. This is computationally very efficient. We also utilize the symmetry plane at the horizontal center of the target formation. The wellbore is tilted for illustrational purposes only. The numbers refer to the ethyl acetate concentration in mol/m^3 at the end of shut-in in one of our models.

The first SWCT test results were published by Tomich et al. (1973). A SWCT test samples a large rock volume around the well, takes relatively short time (typically 2–3 weeks) and is quite robust to near-well formation damage noise. SWCT tests may yield 'fair to excellent estimates of S_{or}' in both sandstone and carbonate reservoirs with large variations in temperature, fluid salinity and rock properties (Chang et al., 1988). An accuracy of about 2–3% is suggested by laboratory results from pressure-core methods under favorable circumstances according to Tomich et al. (1973).

Which primary tracer is found suitable for a particular reservoir depends primarily on the reservoir temperature. Ester acetates are normally employed in high temperature (above about 50 °C) reservoirs whereas formates are preferable at lower temperatures (Deans and Majoros, 1980; Mechergui et al., 2012). The most widely used primary tracer is probably ethyl acetate. Of the 59 tests discussed by Deans and Majoros (1980), 41 (70%) used ethyl acetate as the primary tracer. In a recent paper, Doorwar et al. (2020) discuss 55 published SWCT tests – 44 (80%) of them used ethyl acetate. In this contribution, we focus on ethyl acetate as the primary tracer.

2. Temperature gradients and pH changes

There are two potentially important mechanisms that almost universally are ignored in the planning and interpretation of SWCT tests. The first is that a temperature gradient may develop across the primary tracer bank (Park, 1989). Since the hydrolysis rate of the primary tracer increases exponentially with temperature, such a gradient will cause the secondary tracer to be located further away from the wellbore than the primary tracer is. During the production phase, this 'handicap' will reduce the observed time difference between the primary and secondary tracers and this will translate into a too low S_{or} estimate if the effect isn't accounted for (Park, 1989; Park et al., 1991; Pedersen, 2018, 2021). Reservoir cooling was discussed by Skrettingland et al. (2010) and Khaledialidusti et al. (2015) on the Snorre field, but then only as an average temperature. They therefore did not consider the S_{or} error a temperature *gradient* can produce. Temperature changes in the target formation will also affect the distribution constant of the partitioning primary tracer and thus the S_{or} estimates regardless of which method is used in their calculation. To avoid cooling of the oil-bearing formation altogether would seem to require an infinitely low injection rate and thus an infinitely long injection period. However, whether cooling has a significant effect is another question. Park et al. (1991) developed mathematical criteria for when a temperature gradient across the primary tracer bank has a significant bearing on S_{or} estimates. They provide easy to use graphical solutions that can be used to assess qualitatively whether nonisothermal effects may be important or not. Quantitative results, however, require modelling. Pedersen (2018) demonstrated by computer simulations how hypothetical temperature sensitive fluorescent nanotracers co-injected with the primary tracer might help constrain SWCT temperatures and thus also S_{or} estimates. Wellington and Richardson (1994a) developed an alternative SWCT method where

the primary tracer is a water tracer (halogen-organic acid salts) that is partly converted into a secondary partitioning tracer (CO_2). Unreacted primary tracer or methanol, tritium, etc. may be used as water tracers. This method has several advantages (Wellington and Richardson, 1994a,b,c; Khaledialidusti et al., 2014) but has not been much used. The most important reason is probably that CO_2 is found naturally in many reservoirs and may obscure the signal from the CO_2 tracer. Notwithstanding, this method avoids the 'temperature gradient problem' since the primary tracer moves with the water, i.e., faster than the temperature gradient that typically moves approximately like the oil-water partitioning tracer (Park, 1989).

The second mostly disregarded mechanism is that in addition to the secondary tracer, hydrolysis of ethyl acetate will generate an acid, and this causes a reduction in pH and changes the hydrolysis rate because of the latter's pH-dependence (Wellington and Richardson, 1994b). Wellington and Richardson (1994b) estimate that for a SWCT test in a carbonate-cemented California turbidite as well as in a Gulf Coast sandstone, most of the secondary tracer (ethanol) was generated during transit (injection and production), and not during shut-in. This may violate a basic tenet in the SWCT method (cf. Deans and Majoros, 1980), namely that most of the ethanol is produced during shut-in. They estimated that in the carbonate-cemented California turbidite, S_{or} was increased from about 20 to 40% when pH-driven hydrolysis rate changes of ethyl acetate are accounted for. A CO_2 SWCT test yielded 41% (Wellington and Richardson, 1994c), i.e., very close to the 'pH-corrected' ethyl acetate result. Wellington and Richardson (1994c) warn, however, that in their opinion, the pH-corrected ethyl result 'cannot be used for corroboration because of excessive tracer generation during transit' and consequently poor S_{or} resolution. On the other hand, Deans and Ghosh (1994) also modeled the carbonate-cemented turbidite SWCT test and they concluded that although pH effects did increase the volumes of ethanol produced during injection and production at the expense of that produced during shut-in, this did not much influence the S_{or} estimate (25%, or less if cross-flow and other complexities are included). In the Gulf Coast sandstone, the pH corrected ethyl acetate and the CO_2 methods yield similar results (Wellington and Richardson, 1994c). Relatively little work has subsequently been published on the effect of pH changes on S_{or} estimates. The work by Khaledialidusti and Kleppe (2018) represents an exception. They discuss 1D (single and two-phase) isothermal (consequently no temperature gradients) SWCT models that incorporate pH changes and their effect on hydrolysis rates and tracer concentrations. In addition, they discuss two specific cases – one is the California Turbidite case earlier presented by Deans and Ghosh (1994), the other is what they call a 'General Sandstone Reservoir' that is lean in calcite cement and has an 'intermediate' brine buffer capacity. However, Khaledialidusti and Kleppe (2018) present tracer production curves only for the latter model and they provide no S_{or} estimates. More than twenty-five years ago, Deans and Ghosh (1994) concluded: 'future efforts to interpret SWCT tests will definitely be more credible if pH dependence of hydrolysis rate is included.' Judging from the SWCT literature, this advice has mostly been overlooked.

The main objective of the work presented here is to study the simultaneous effects of target formation cooling and primary tracer hydrolysis rate pH dependence on S_{or} estimates from SWCT tests when buffering by minerals in the target formation or chemical species in the injected brine are accounted for. This contribution is a continuation of the work presented in Pedersen (2021) who, however, did not include pH buffering. We also include an improved (relative to Park (1989), Park et al. (1991) and Pedersen (2021)) thermal conductivity model of the oil-bearing formation, as well as provide results on the relative degree of hydrolysis pre-, syn- and post shut-in. Our SWCT model is the first ever to include temperature gradients and pH changes taking into account buffering.

3. Model and data

The temperature model presented in Park (1989) is our starting point. Fluid flow is assumed to be radial from and towards the wellbore during injection and production, respectively. This makes it feasible to have an axially symmetric model centered on the vertical wellbore (Fig. 1). Model parameters and values are given in Table 1.

In this manner, three-dimensional effects are accounted for in a mathematically simple and computationally efficient manner. The wellbore is surrounded by three horizontal rock units. The formation where we estimate S_{or}, i.e., the target for the SWCT test, is a permeable rock. Two impermeable shales with equal thicknesses are found above and beneath the target formation. We assume, like Park (1989) and Park et al. (1991) that the target formation and the adjacent impermeable layers are at thermal equilibrium (T≡TR) when the calculations commence (Fig. 2). This is realistic due to the small depth interval (typically a few tens of meters) provided the rocks have not been thermally disturbed by for instance a previous SWCT test or a waterflood to reduce oil saturation to residual. All model parameters (except brine composition; see Table 2) and their values are given in Table 1.

Table 1
Symbols, values and descriptions.

Symbol	Value	Description
H	12 m	Target formation height
W	10 m	Model width
r		Radial distance from center of wellbore
Qinj	450 bls/d	Injection rate
Qprod	480 bls/d	Production rate
C		Concentration
C_I	See Table 2	Injection concentration
C_R	See Table 2	Reservoir concentration
D_F	10^{-9} m^2/s	Diffusivity
T		Temperature
T_I	See Fig. 2	Injection temperature
T_R	73 °C	Initial reservoir temperature
Tinj	1 d	Injection period
Tpush	1 d	Push period
tshutin	6 d	Shut-in period
Tprod	6 d	Production period
φ	23%	Target formation porosity
φ_{eff}	18%	Effective porosity
φ_{sh}	29%	Shale porosity
k	See text	Ethyl acetate hydrolysis rate
Sor	22%	Residual oil saturation
S_{or}*		Estimated S_{or} using Eq. (23)
S_{or}**		Estimated S_{or} using Eq. (25)
S	20 000 ppm	Salinity
u	Eq. (1)	Darcy velocity
v	u/effective porosity	Interstitial velocity
$(\rho C_p)_{oil}$	1.67 10^6 J/m^3/K	Oil volumetric heat capacity
$(\rho C_p)_{rock}$	2.41 10^6 J/m^3/K	Rock volumetric heat capacity
$(\rho C_p)_{water}$	4.18 10^6 J/m^3/K	Water volumetric heat capacity
$k_{m,sandstone}$	3.00 W/m/K	Sandstone matrix thermal conductivity
$k_{m,shale}$	2.45 W/m/K	Shale matrix thermal conductivity
k_o	0.12 W/m/K	Oil thermal conductivity
k_w	0.6 W/m/K	Water thermal conductivity
A	0.021 K/m	Geothermal gradient
Z	3000 m	Depth to target formation
B	10 °C	Earth's surface temperature
T_0	10 °C	Water surface temperature
Cp	4180 J/K/kg	Water specific heat
r_0	0.1 m	Well radius
A	1.1 10^{-6} m^2/s	Thermal diffusivity of the Earth
α_r	10^{-3} m^2/s	Radial dispersivity
α_z	0.5 α_r	Vertical dispersivity
U		Fluid velocity in wellbore

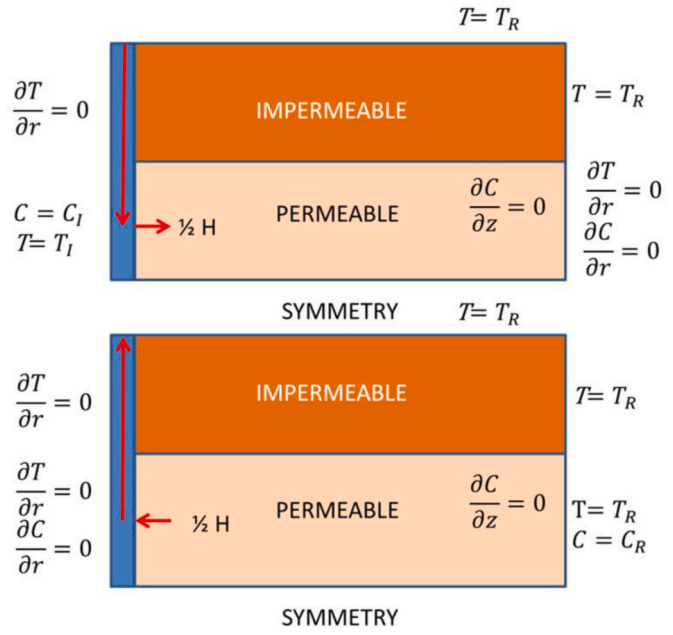

Fig. 2. Boundary conditions during injection (upper), shut-in and production (lower). Modified from Park (1989).

3.1. Fluid velocity

The injected brine flows into the permeable layer from the left (Fig. 2). For perfect radial flow of an incompressible fluid, the Darcy velocity $\vec{u}$, as a function of distance, r, from the center of the wellbore is (e.g., Park, 1989):

$$\vec{u} = \begin{pmatrix} u_r \\ u_z \end{pmatrix} = \begin{pmatrix} \frac{Q}{2\pi Hr} \\ 0 \end{pmatrix} \quad (1)$$

in which Q is the pumping rate, H the thickness of the permeable layer and r is distance from the wellbore center.

3.2. Temperature calculations

The temperature, T, is calculated by solving the heat equation:

$$(\rho C_p)_{eff} \frac{\partial T}{\partial t} + (\rho C_p)_w \vec{u} \nabla T = \nabla (k_{eff} \nabla T) \quad (2)$$

in which the effective volumetric heat capacity is:

$$(\rho C_p)_{eff} = \varphi \{(\rho C_P)_o S_{or} + (\rho C_P)_w S_w\} + (1-\varphi)(\rho C_P)_r \quad (3)$$

where the subscripts *or*, *w* and *r* refer to residual oil, water and rock, respectively, φ is rock porosity, and S is saturation. In a two-phase system, we have that

$$S_w = 1 - S_{or} \quad (4)$$

$k_{eff,i}$ is the effective thermal conductivity:

$$k_{eff,i} = \varphi \{k_o S_{or} + k_w S_w\} + (1-\varphi) k_{m,i} \quad (5)$$

in which *i* represents the sandstone target formation or the shales above and beneath it, k_o and k_w are the thermal conductivity of oil and water, respectively, and $k_{m,i}$ is the matrix thermal conductivity of sandstone or shale. The hydrolysis reaction of ethyl acetate is slightly exothermic, but with the tracer concentrations used in SWCT tests, its effect on temperature can be ignored.

3.3. Injection temperature

For a wellbore-rock system initially at thermal equilibrium, Ramey (1962) derived an approximate expression for the brine temperature in the wellbore as a function of depth, z, and time, t:

$$T(z,t) = az + b - aA + (T_0 + aA - b) exp\left(-\frac{z}{A}\right) \quad (6)$$

in which z is depth, a is the geothermal gradient of the Earth, b is the surface geothermal temperature, and T_0 is the surface temperature of the injected brine. For water injection down casing,

$$A = \frac{WCpf(t)}{2\pi k} \quad (7)$$

where W is the injection rate measured in kg s^{-1}, C_p is the specific heat of the injected fluid and k is the thermal conductivity of the Earth. More complex expressions exist for other wellbore configurations. The function f is depicted in Ramey (1962) (his Fig. 1 – 'cylindrical source'). Fig. 3 illustrates the brine temperature as a function of time with the parameters in Table 1. It takes the tracer slug approximately 1.3 days to reach the target formation at 3 km depth and the tracer starts to flow into the target formation. The temperature depicted in Fig. 3 is used as the injection temperature TI (cf. Fig. 2) in the simulations.

Parameter values are given in Table 1 and boundary conditions in Fig. 2.

The perhaps most important feature in that figure is that there is a smooth decrease in the temperature of the injection fluid with time. If we had used an abrupt temperature change like for example Park et al. (1991) did, our simulations show that it would have been difficult to avoid using unrealistically high dispersivity values to stabilize the combined temperature and pH dependent hydrolysis rate numerical calculations. Most important is that such a smooth temperature change would appear to be more realistic. Pedersen (2018) demonstrates how properly designed fluorescent nanoparticles co-injected with the primary tracer can yield information on the real temperature history during a SWCT test.

3.4. Chemical reactions and solute transport

Ethyl acetate hydrolyzes to produce ethanol and acetic acid:

$$Ethyl\ Acetate + H_2O \rightarrow Ethanol + Acetic\ Acid \quad (8)$$

In addition, there are several equilibrium reactions:

$$Acetic\ Acid \leftrightarrow H^+ + Acetate\ Ion^- \quad (9)$$

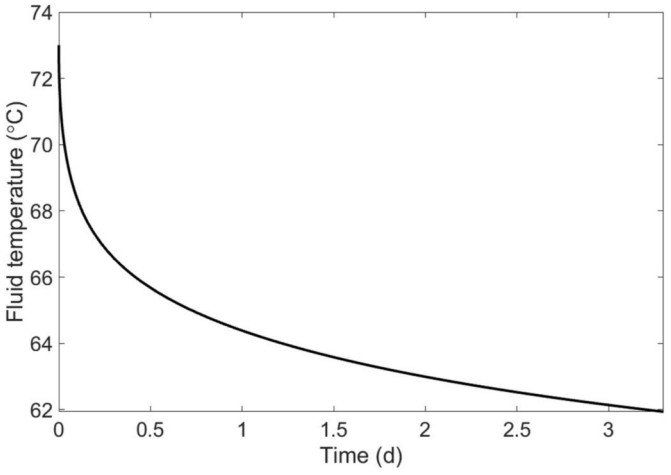

Fig. 3. Injection temperature as function of time derived from Eqs, 6–7 with the parameters in Table 1.

with the equilibrium constant, K_{eq} (for concentrations in mole l^{-1} (i.e., M) – in the simulations we use the SI unit mole m^{-3}):

$$K_{eq} = 1.8\ 10^{-5} \tag{10}$$

and the dissociation of water equilibrium reaction:

$$H_20 \leftrightarrow H^+ + OH^- \tag{11}$$

The water dissociation constant, K_W,

$$K_W = [H^+][OH^-] \tag{12}$$

depends on temperature (Fig. 4).

The ethyl acetate concentration in the injected brine (C_I) is 40 mol/m^3 (=0.04 M) (cf. Fig. 2).

The buffering due to carbonate species is modeled by three equilibrium reactions (Deans and Ghosh, 1994):

$$H_2CO_3 \leftrightarrow H^+ + HCO_3^- \tag{13}$$

$$HCO_3^- \leftrightarrow H^+ + CO_3^{--} \tag{14}$$

$$CaCO_3(s) \leftrightarrow Ca^{++} + CO_3^{--} \tag{15}$$

The equilibrium constants for the first two reactions at the reservoir conditions are $10^{-6.4}$ and $10^{-10.3}$, respectively, and the solubility product of calcite is $10^{-8.3}$ (Plummer and Busenberg, 1982).

The transport of the various chemical species in the target formation is described by the equation:

$$(\varphi_{eff} + \rho_b k_{P,i})\frac{\partial C_i}{\partial t} + \vec{u}\nabla C_i = \nabla\left[\left(D_{D,i} + \frac{\varphi_{eff}}{\tau_i}D_{F,i}\right)\nabla C_i\right] + \varphi_{eff}R_i \tag{16}$$

Here, φ_{eff} is the effective porosity equal to $\varphi(1 - S_{or})$, ρ_b is the dry bulk density, $k_{P,i}$ is the adsorption isotherm, C is the concentration, $D_{D,i}$ is the dispersion, τ_i is the tortuosity, $D_{F,i}$ is the diffusivity, R_i is a reaction term and i refers to solute number i. For ethyl acetate $R = -kC_{ethyl\ acetate}$, whereas for ethanol and acetic acid, $R = kC_{ethyl\ acetate}$. The adsorption isotherm is

$$k_P = \frac{S_{or}\varphi\ K}{\rho_r(1-\varphi)} \tag{17}$$

for ethyl acetate and zero for the other solutes. K is the distribution constant (partitioning coefficient), ρ_r is rock density and the other terms have been defined earlier. We use the following expression for K (Deans and Majoros, 1980):

$$K = \left\{2.4 + \left(1.0 + \frac{S_s}{24,000}\right)(0.018T - 5.197)\right\} \tag{18}$$

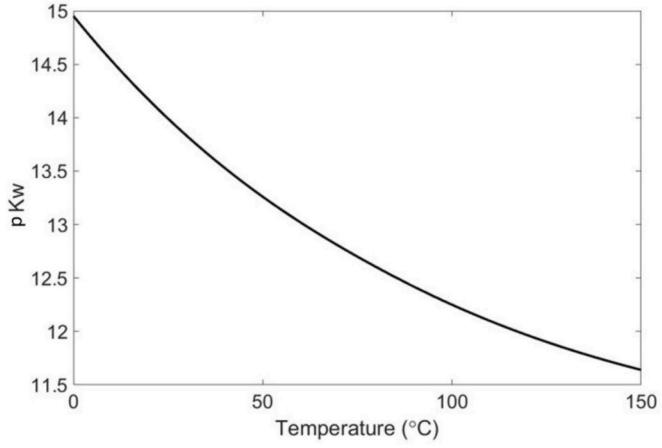

Fig. 4. pKw as a function of temperature. Based on Bandura and Lvov (2006).

where we have neglected K's dependency on the tracer concentration because this effect is small (Deans and Majoros, 1980). S_s is salinity measured in ppm while temperature is measured in Kelvin. The boundary conditions for the solute transport calculations are given in Fig. 2.

The overall reaction rate for the hydrolysis of ethyl acetate to ethanol, k, depends on $[H^+]$ and $[OH^-]$ (International Critical Tables first edition, 1930):

$$k = k_a[H^+] + k_b[OH^-] \tag{19}$$

in which k_a and k_b are the acid and base catalysis factors, respectively. Fig. 5 illustrates k (note the logarithmic scale) as a function of pH and temperature. We note that the hydrolysis rate minimum depends on temperature.

The much used pH independent expression for the hydrolysis rate of ethyl acetate per day, kh, published by Deans and Majoros (1980), reads:

$$log_{10}(kh) = 8.6 - \frac{3469}{T} \tag{20}$$

where T is in K is used for comparison.

We calculate the tortuosity in the target formation from the Millington and Quirk (1961) formula $\tau = \varphi^{-1/3}$. For the porosity in Table 1, this yields 1.6. Dispersion is calculated from the expressions (Bear, 1979):

$$D_{Dr} = \alpha_r\frac{u_r^2}{|u|} \tag{21}$$

and

$$D_{Dz} = (\alpha_r - \alpha_z)\frac{u_z^2}{|u|} \tag{22}$$

where α_r and α_z are the radial and vertical dispersivities, respectively. See Table 1 for parameter values.

The set of equations above are solved using the commercial finite element PDE software COMSOL Multiphysics (2018). The mesh consists of triangular elements with higher resolution near the wellbore because that is where most of the variations take place. Time stepping is performed by a second order implicit backward differentiation formula (BDF). It takes typically between five and 10 min to solve a model on a 64 bit computer with two processors and 128 GB RAM memory.

The most important difference between our chemistry model and the models published by Khaledialidusti and Kleppe (2018) is probably that we have a realistic 3D description of the temperature changes during a SWCT test whereas their models are isothermal. That the assumption of

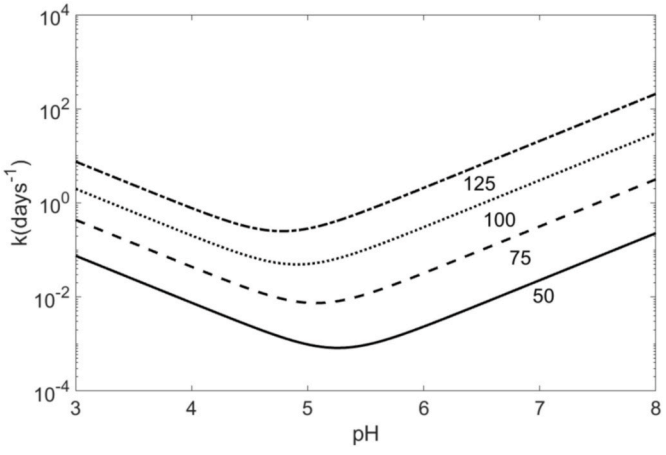

Fig. 5. Hydrolysis rate constant of ethyl acetate as function of pH and temperature in °C. Based on International Critical Tables (1930) and pKw (Fig. 4).

constant temperature during a SWCT test is almost universally used in the literature on SWCT tests does not make it any more realistic. Because temperature governs the hydrolysis rate of ethyl acetate and other esters, induced pH changes and distribution constants, a sound model of temperature changes during a SWCT test is important. The 'handicap' (horizontal separation between the ethyl acetate and ethanol tracer curves when production commences) identified already by Park and co-workers around 1990 cannot be studied in isothermal models. Furthermore, our model has a radial velocity field representative for (most) SWCT tests while Khaledialidusti and Kleppe (2018) use a 1D transport equation. We also consider diffusivity and dispersion. These effects were ignored by Khaledialidusti and Kleppe (2018).

3.5. Test, brine and formation rock data

As in Pedersen (2021), we define a generic or representative (approximate arithmetic averages) SWCT test and rock data set (Table 1) based on Tables 5-1 in Deans and Majoros (1980). Their table contains data from 59 SWCT tests mostly in sandstones although a few limestone cases are included as well. We only consider the common ethyl acetate primary tracer.

We define four simulation models (Table 2). They are based on Ghosh (1994) but slightly modified to be consistent with the model parameters in Table 1.

Model 1 may represent a sandstone with calcite cement. In Model 2, also with calcite cement, the brine has less calcium but more bicarbonate and lower pH than Model 1. Model 3 is a clean sandstone without calcite cement and the brine contains no calcium but much bicarbonate. Model 4 has no buffer capacity neither in the brine nor in the target formation. Although we discuss only four models, they are quite different and represent an important subset of the realistic SWCT test parameter space. Future work should investigate also other buffer models.

3.6. Sor estimates

S_{or} is estimated from the synthetic tracer concentration curves using two methods. The first is the direct application of Cook's (1971) chromatography formula:

$$S_{or}^{*} = \frac{t_{Etyl\ Acetate} - t_{Ethanol}}{t_{Etyl\ Acetate} + t_{Ethanol}(K-1)} \tag{23}$$

in which t is the time when the concentrations of ethyl acetate or ethanol are at their maximum and K is again the distribution constant.

One of the assumptions in Eq. (23) is that dispersion of the tracers is negligible. In a real SWCT test, there will be dispersion. Deans and Majoros (1980) suggested to use the ratio between the first and zero statistical moments (i.e., the mean residence time) defined as

$$\overline{t_i} = \frac{\int_0^\infty t\, C_i dt}{\int_o^\infty C_i dt} \tag{24}$$

to account for dispersion in SWCT tests; *i* stands for ethyl acetate or ethanol. The estimated value of S_{or}** is obtained by inserting the times from Eq. (24) into Eq. (23), i.e.,

$$S_{or}^{**} = \frac{\overline{t_{Etyl\ Acetate}} - \overline{t_{Ethanol}}}{\overline{t_{Etyl\ Acetate}} + \overline{t_{Ethanol}}(K-1)} \tag{25}$$

We use the distribution constant (Eq. (18)) with the reservoir temperature TR in Eqs. (23) and (25). That is the only temperature value available without performing temperature calculations. Pedersen (2021) demonstrated that in some SWCT synthetic tests the simple Eq. (23) may yield better estimates than Eq. (25). We do not mean to suggest that Eqs. (23) and (25) are the best ways to obtain good S_{or} estimates. However, they are much used – perhaps more than any others.

Table 2
Brine composition (mol/m^3) and pH in the four buffer models. Models 1 and 2 include calcite in the target formation.

Model	C_I	Ca^{++}	CO_3^{--}	HCO_3^-	H_2CO_3	pH
1	40	1500	$3.34\ 10^{-6}$	0.0035	$4.62\ 10^{-4}$	7.3
2	40	3.74	0.00134	7.49	5.26	6.55
3	40	0	0.18	206.8	29.79	7.24
4	40	0	0	0	0	6.34

4. Results

Fig. 6 illustrates how pH and k change with time in a vial (small glass, plastic vessel or bottle) due to hydrolyses of ethyl acetate with the compositions in Table 2.

The vial is kept at a constant temperature of 73 °C, i.e., the reservoir temperature, TR, and there is no oil in it. Such models are useful for understanding the chemistry of a SWCT test but ignore any interaction (temperature, partitioning, dispersion) between the injected fluids and the rocks surrounding the wellbore except from the calcite 'cement' in Models 1 and 2. We observe in Fig. 6.1 (Model 1) that after less than one day, the pH has dropped below 6 and the hydrolysis rate is reduced by a factor of about 25. In Model 2 (Fig. 6.2), there is only a small fall in pH and the hydrolysis rate is reduced by about 50% after six days. In Fig. 6.3 (Model 3, i.e., the model without calcite 'cement' but very high in bicarbonate), there is again only a minor reduction in pH and k is only decreased by approximately 50%. Finally, Fig. 6.4 (Model 4, i.e., the 'no-buffer' case with no buffer capacity in neither the injected brine nor in the rock), demonstrates a very rapid pH reduction beyond the hydrolysis rate minimum point in Fig. 5, after which the hydrolysis rate increases and eventually surpasses its initial value. These simple vial simulations indicate that when we now include interactions between injected brines and the rocks surrounding the wellbore, a quite complex picture may be expected.

The vial model results in Fig. 6 ignore the effects of injecting the various brines into the porous target formation surrounding the wellbore and leaving them there to hydrolyze, as well as the cooling caused by the relatively cold brine.

Fig. 7 illustrates pH and temperature as functions of distance from the well bore center, r, at the end of shut-in for the SWCT model in Fig. 1. The pH minima are close to those seen in Fig. 6. This suggests that at least in some cases, the minimum pH may be estimated by a simple vial model. The temperature curves are all the same because the thermal properties of the brine do not change due to the small variations in brine composition or tracer concentrations. Far from the wellbore, i.e., r larger than approximately 5 m, the temperature equals the initial reservoir temperature; TR. Approaching the wellbore, the temperature tapers off until it reaches the wellbore temperature shown in Fig. 3. The pH reductions observed in Fig. 7.1 and 7.4 are not only much larger than in Fig. 7.2 and 7.3, but also much wider and will thus affect the ethyl acetate hydrolysis more substantially.

The hydrolysis rate, k (cf., Fig. 5), and the commonly used pH independent rate, kh (Deans and Majoros, 1980), are presented in Fig. 8 for the pH and temperature data in Fig. 7. For the latter, we use the reservoir temperature since that is the only temperature that is available without temperature calculations. In Fig. 8.1, we see a dramatic reduction in k since a pH value of about 5.5 (Fig. 7.1) yields the minimum hydrolysis rate (Fig. 5). The rate is also much lower than the much used pH independent rate, kh. Designing SWCT tests using the kh may thus underestimate the time required to obtain a certain degree of hydrolyses in rocks with calcite, or other carbonates, with the Model 1 brine composition. Also, in Models 2 and 3 (Fig. 8.2 and 8.3, respectively) we note that k is lower than kh, but the difference is much smaller than for Model 1. In Fig. 8.4 (Model 4) we observe a more complicated k

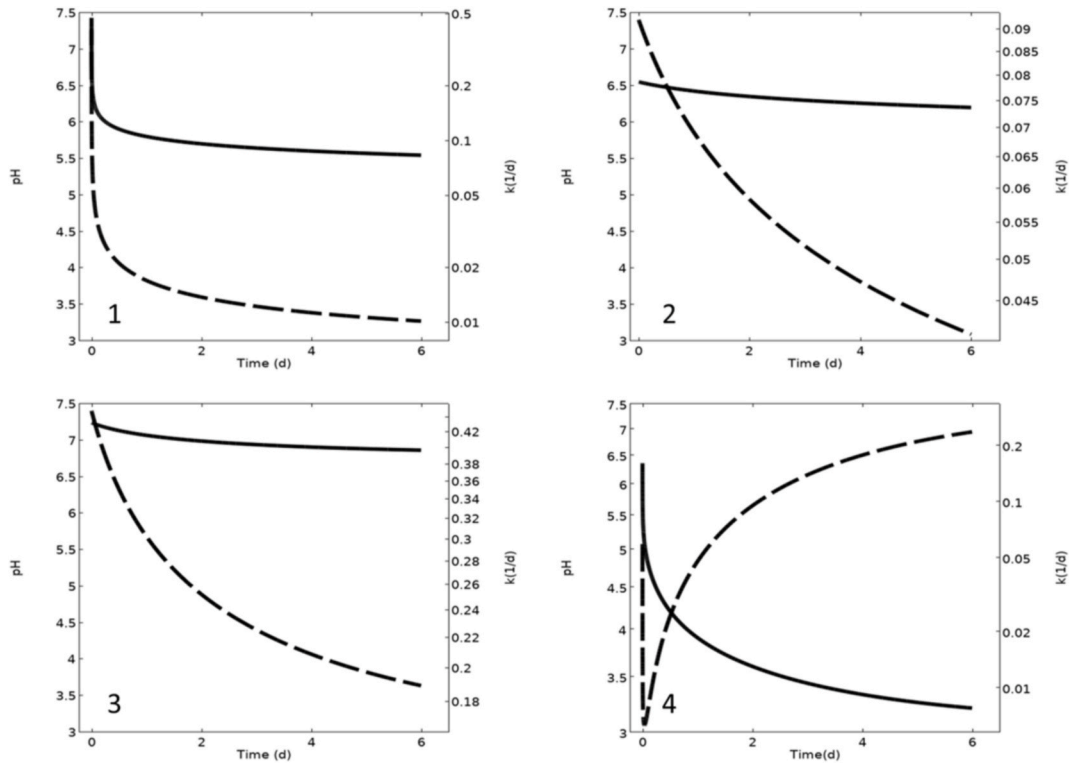

Fig. 6. pH (solid) and k (dashed) as functions of time in the vial models. 1: Model 1. 2: Model 2. 3: Model 3. 4: Model 4.

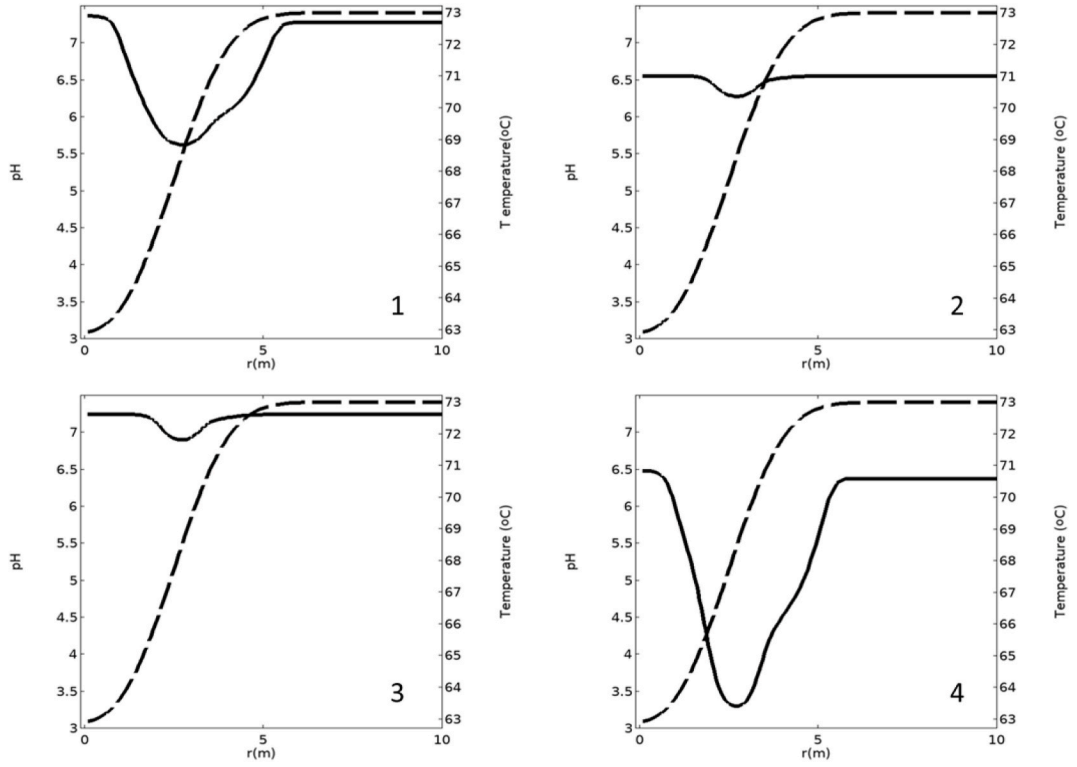

Fig. 7. pH (solid) and temperature (dashed) as a function of distance from the wellbore center at the end of shut-in. 1: Model 1. 2: Model 2. 3: Model 3. 4: Model 4.

curve. This is because with the pH values in Fig. 7.4, the hydrolysis rate passes through its minimum (Fig. 5) and then increases as pH continues to fall.

Fig. 9 shows the calculated ethyl acetate and ethanol concentrations at end of shut-in for the four models in Table 2. In all four displays, we note that the ethanol curves are slightly displaced to the right relative to the ethyl acetate curves. This is the 'handicap' discovered by Park (1989) and Park et al. (1991). For Model 1, only a small fraction of the ethyl acetate has been converted into ethanol. This is because with Model 1 the hydrolysis rate is close to its minimum (Fig. 5). For Model 2,

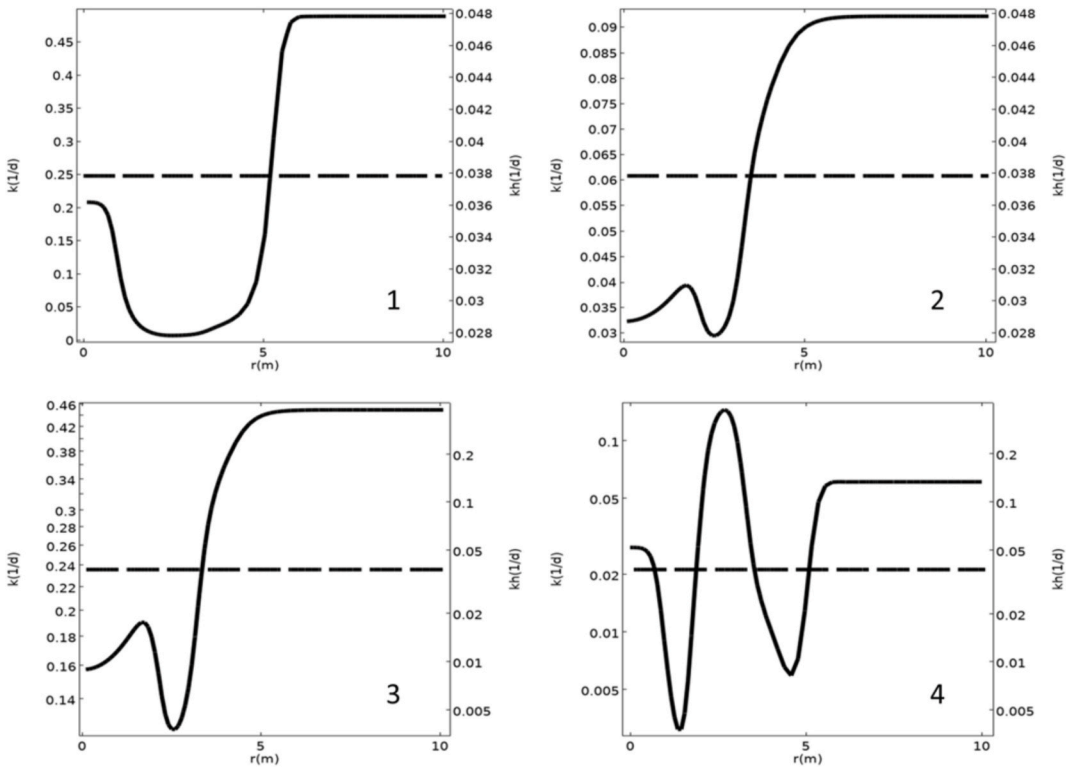

Fig. 8. k (solid) and kh (dashed) as function of distance at the end of shut-in for Models 1 to 4.

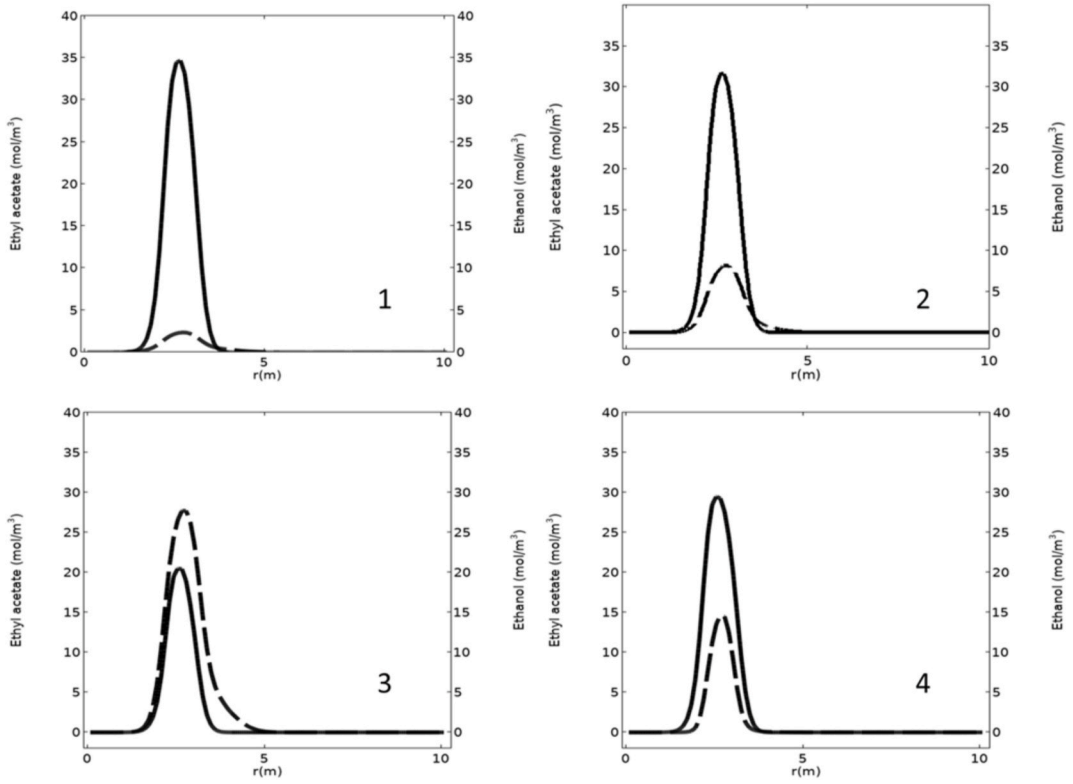

Fig. 9. Ethyl acetate (solid) and ethanol (dashed) concentrations as functions of position at the end of shut-in (9.3 d) for Models 1 to 4.

the rate is higher and consequently more ethanol has been generated. With Model 3, we note that more than 50% of the ethyl acetate has been hydrolyzed. Finally, Model 4 yields a degree of hydrolysis between Models 2 and 3, congruent with the hydrolysis rates in Fig. 8.

The ethyl acetate and ethanol production curves are illustrated in Fig. 10 together with the Sor* and Sor** estimates (Eqs. (23) and (25)). We see that S_{or}* and S_{or}** underestimate the true S_{or} (22%) value by 3–5% and 3–11% (saturation units), respectively.

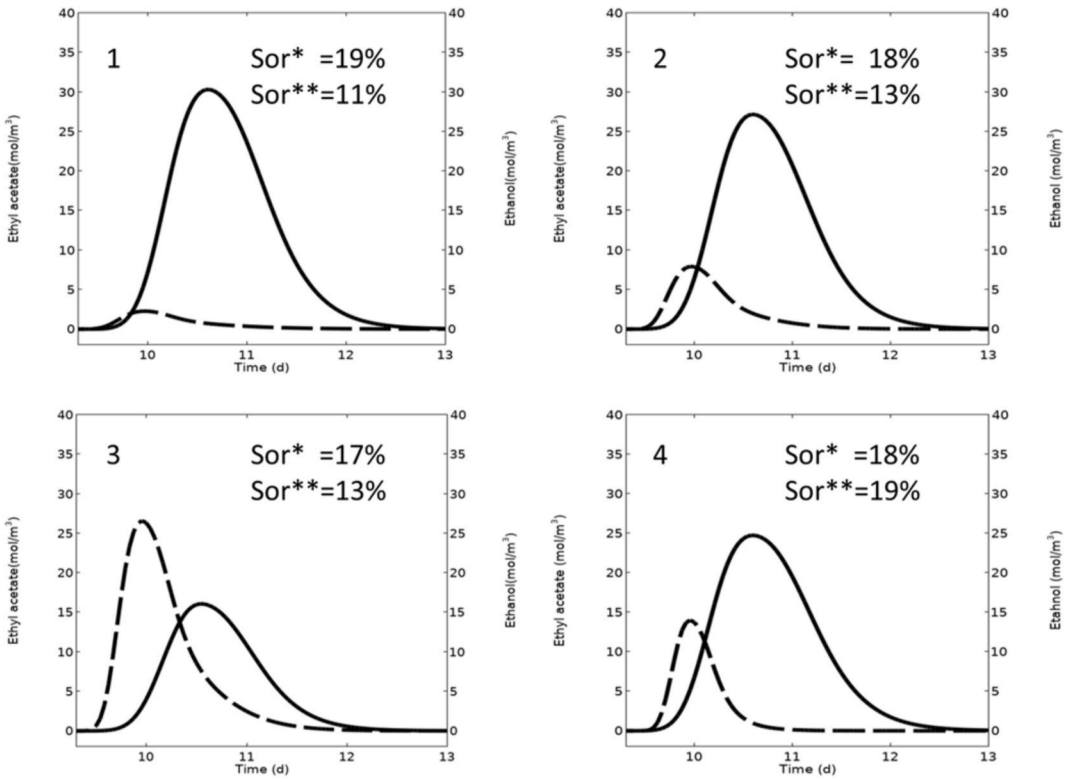

Fig. 10. Produced ethyl acetate (solid) and ethanol (dashed) concentration curves. Sor* and Sor** are the Sor estimates with Eqs. (23) and (25), respectively.

5. Discussion

Judging from Figs. 6–8, it is difficult to define a meaningful 'average' rate of hydrolysis in any of the four models discussed in this contribution since the rate changes considerably in space as well as with time. Our four models span a relatively large SWCT test parameter space and we would thus argue that this also pertains to many real SWCT tests. Hydrolysis rate variations should be included already in the planning phase of the test. Using Eq. (19) (Fig. 5) or other T-pH models is quite straightforward, and there is not much reason in our opinion to use some 'average' rate of hydrolysis. To fully exploit such more realistic rate expressions requires, however, solving for temperature as well as pH changes during the SWCT test. Overestimating the time required for sufficient hydrolysis to take place costs money. It may also lead to there being not sufficient primary tracer left to observe. A too short shut-in may lead to poor S_{or} estimates because of an insufficient secondary tracer concentration.

Fig. 11.1 illustrates the relative percentages of ethyl acetate converted into ethanol for the pre-, syn- and post-shut-in periods for Models 1–4. We find that in all four models, the fraction of ethyl acetate that hydrolyzes during shut-in is higher than the minimum 50% recommended by Deans and Majoros (1980). In other words, we do not observe that the generation of ethanol during transit (i.e., injection + production) overshadows the generation during shut-in as did Wellington and Richardson (1994b) in their SWCT model of a carbonate cemented California turbidite and a Gulf Cost sandstone. We believe that the principal reason for this difference is the difference in modelling methodology. Whereas we solve the conservations laws for energy (temperature; Eq. (2)) and mass (transport of dilute chemical species; Eq. (16)) and use the calculated temperature and pH to define the rate of hydrolysis by Eq. (19), Wellington and Richardson (1994b) use the observed pH values (in the produced fluid) to estimate average hydrolysis rates for injection, shut-in and production. Although they include ethyl acetate hydrolysis also in the tubing during production (which we do not), this probably cannot explain the difference because once the ethyl acetate enters the tubing, it will start to cool on its way towards the surface and quite rapidly hydrolysis should become very slow. In addition, Wellington and Richardson (1994b) do not consider the temperature gradient across the primary tracer bank. Further work would be required to investigate this matter more deeply.

That S_{or}** may yield poorer residual saturation estimates than S_{or}* was also discovered by Pedersen (2021) in a study of SWCT tests without buffering in neither the formation rock nor in the injected brine. We suggest the following explanation for this phenomenon. The temperature gradient across the primary tracer bank in concert with pH-driven rate changes cause the secondary tracer profile to have a more distorted shape (larger deviation from the ideal Gaussian) than the 'rest' primary tracer has. Wellington and Richardson (1994b) proposed that the distorted shape of the secondary tracer (ethanol) curve in a California turbidite SWCT test was a consequence of most ethanol being generated during transit. Our study does not support this explanation since most of the secondary tracer (63%) in Model 3 was produced during shut-in (Fig. 11a). Anyway, since all the secondary tracer has been produced under such conditions, whereas the rest primary tracer is what remains of a more ideal shape. In Fig. 11.2, we again see the production curves for Model 3 as well as the Sor* and Sor** estimates. Also illustrated are the elapsed times relative to start of production (9.3 d) for the ethyl acetate ('p' for primary) and ethanol ('s' for secondary) tracers. The times are given for the Sor* estimate ('*', i.e., time is defined by the top of the concentration curves) as well as the Sor** estimate ('**', time is defined by Eq. (23)). We note that the effect of applying Eq. (24) is greater for the secondary tracer (0.21 d) than for the primary tracer (0.18 d), and this reduces Sor** relative to Sor*. There does not seem to be much point in pursuing the topic of the relative merits of the Sor* and Sor** estimates, since a straightforward, more transparent and mathematically sounder way forward is simply to use models like the model applied in this paper. Such models can also be refined to include more physical and chemical processes as well as more complicated rock geometries and properties like dual porosity, fracture and faults, coarsening, diagenetic effects, and so on and so forth.

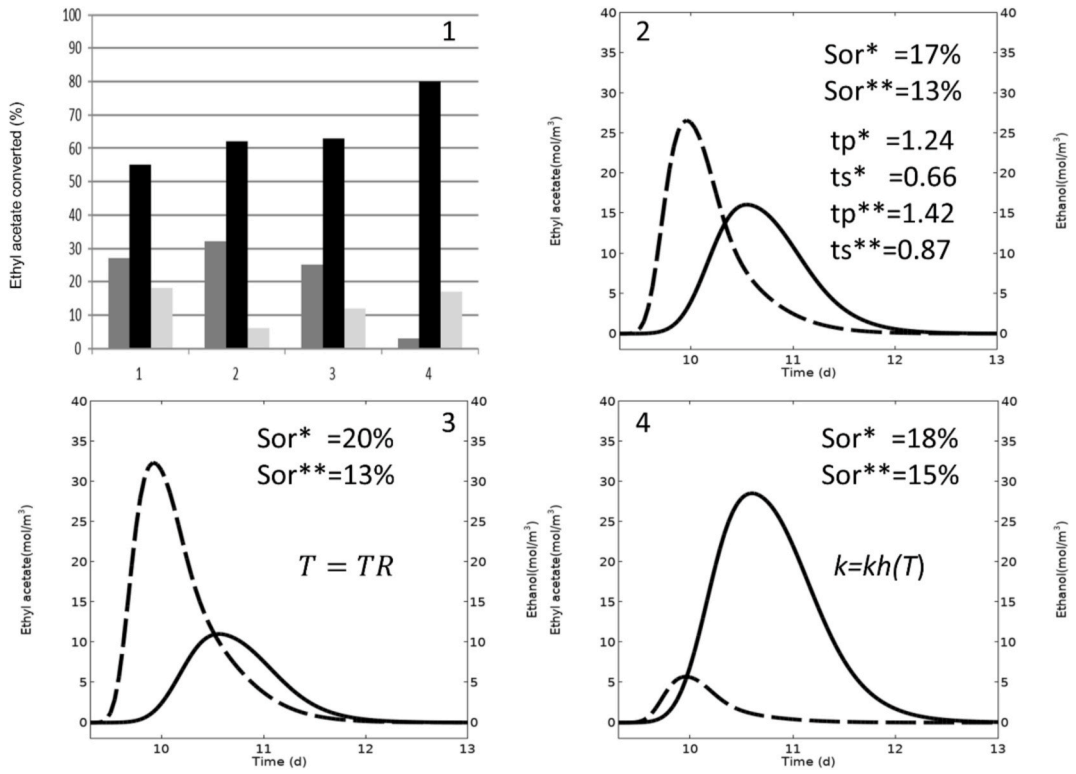

Fig. 11. 1 Relative percentage of ethyl acetate converted to ethanol during pre- (dark grey), syn- (black) and post-shut-in (light grey). 2. Concentration of produced ethyl acetate (solid) and ethanol (dashed) as functions of time. Included are also the times since production started for ethyl acetate ('p') and ethanol ('s') with times defines by top of peak concentration ('*', Eq. (23)) and mean residence time ('**'; Eq. (25)). 3. Ethyl acetate and ethanol concentrations as functions of time for an isothermal model with temperature equal to the reservoir temperature, TR. Also shown are the Sor* and Sor** estimates of S_{or}. 4. Ethyl acetate and ethanol concentrations as functions of time for the kh hydrolysis rate model (Eq. (20)).

Fig. 11.3 depicts synthetic production in the case that the reservoir temperature is constant. In this scenario, there will be no temperature gradient 'handicap', and the Sor* estimate is wrong with only1%. If we employ the pH independent hydrolyses model, kh (Eq. (17)), (Fig. 11.4), we arrive at a Sor* estimate equal to 18% and a Sor** estimate of 15%. These relatively large errors are produced by the temperature gradient that is present also when the kh rate is used.

If pH is included in SWCT models implies that there will be one more type of observations available to constrain S_{or}. Fig. 12 depicts pH and ethanol concentration in the produced brine as functions of time for Models 1–4. We note that the pH curve can be utilized as a control of the timing of the peak in the ethanol curve because of their quasi-mirror shapes. Minimizing the weighted difference (least-squares or other measure) between the calculated pH (and potentially other chemical information), primary and secondary tracer concentrations and the observed values using inversion methods (e.g., Aster et al., 2005) should yield improved S_{or} estimates and error estimates. Better test design (e.g., Khaledialidusti and Kleppe, 2017) could be combined with such efforts to bring the SWCT technique forward.

Pedersen (2021) studied temperature gradient and pH effects on S_{or} estimates from SWCT tests assuming no buffer capacity neither in the injected brine nor in the oil-bearing formation. Such a scenario is realistic if the brine contains no significant amounts of chemical species that may buffer the produced acid, and the oil-bearing formation matrix does not contain minerals like calcite that may get in contact with the produced acid and dissolve. Since sandstones almost universally are calcite cemented, the rock type where this 'no buffer' scenario may be most realistic is perhaps in carbonate reservoirs since most of them are oil-wet (Høgnesen et al., 2005) and a veneer of oil may protect the rock from the acid. We propose that this mechanism might be used to obtain not only S_{or} from a SWCT test, but also the effective wettability of the oil-bearing rock surrounding the well. The small figure inside Fig. 12.1 illustrates pH and the ethanol concentration for Model 1 if the calcite in the matrix is shielded from the acid by a veneer of oil. We see that there is a large difference in both pH and ethanol concentration. So if pH (and concentrations of other chemical species as well) was monitored in the produced brine, it should be possible to distinguish between a water-wet and an oil-wet rock. Presumably, a mixed-wettability rock would yield pH and ethanol results somewhere between the curves in Fig. 12.1. Further work is required to investigate this idea.

Al-Abbad et al. (2016) developed a new set of hydrolyzing partitioning primary tracers with much lower quantification limits than the conventional SWCT ester tracers. The primary tracer volumes may thus be reduced by several orders of magnitude. Although not much detail is provided on the new tracers, we anticipate that they should produce only small volumes of acid and give no significant pH reduction. Consequently, the pH-driven hydrolysis rate mechanism should not come into play to any significant degree. Finally, we note that using a water tracer as primary tracer to generate a partitioning secondary tracer (Wellington and Richardson, 1994a), the 'reverse' approach so to speak, avoids or reduces several of the problems discussed in this contribution. In particular, in this scenario there is no temperature gradient across the tracer bank since the water tracer moves well ahead of the temperature gradient (Wellington and Richardson, 199b). Perhaps it would be an idea to develop new primary water tracers with another secondary tracer than CO_2. As discussed above, if the new tracers had been water tracers, the 'temperature gradient problem' should be eliminated or at least much reduced as well.

6. Conclusions

Numerical models that include realistic temperature calculations and

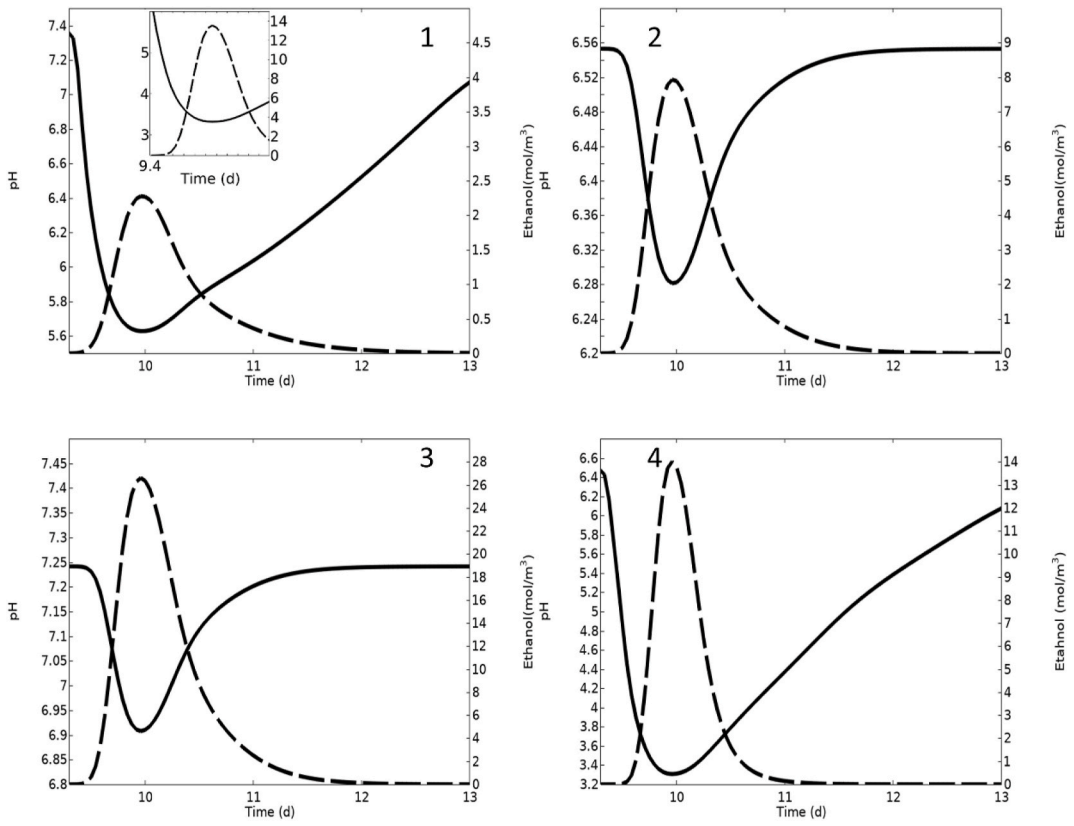

Fig. 12. pH (solid) and ethanol concentration (dashed) in produced brine for Models 1–4. If pH is measured, this information might be used in obtaining an optimum SWCT result. The small figure inside Fig. 12.1 illustrates pH and ethanol concentration in Model 1 if there is no caiclite in the oil-bearing formation. The reduced buffer capacity yields a minimum pH jsut above 3 and a peak ethanol concentration of approximately 13 mol/m^3.

pH-driven primary tracer hydrolysis rate changes are important in the design of SWCT tests and for interpretation of the results.

Simple isothermal vial models provide useful semi-quantitative insight into the chemistry of SWCT tests, but simulation of temperature and chemical species transport in porous media are required for a deeper understanding.

In all four models discussed in this paper, more than 50% of the ethyl acetate hydrolysis occurs during shut-in. Notwithstanding, the 'handicap' caused by the temperature gradient across the primary tracer bank, combined with pH-driven hydrolysis rate changes, violates one of the basic tenants in the conventional Sor estimates; that the primary and secondary tracers start form the same position when production commences.

S_{or} was estimated from the synthetic tracer production curves using the standard chromatographic separation equation as well as with the mean residence time correction. The methods underestimate the true S_{or} value (22%) by 3–5% and 3–11% (saturation units), respectively.

SWCT tests might be used to also estimate the effective wettability at only a moderate extra cost.

New primary hydrolyzing water tracers with very low quantification limits might reduce or even circumvent both the temperature gradient and pH-driven hydrolysis rate changes challenges discussed in this contribution.

Declaration of competing interest

The authors declare that they have no known competing financial interests or personal relationships that could have appeared to influence the work reported in this paper.

Acknowledgements

This work was financed by Institute for Energy Technology (IFE). Comments by Ingegjerd Almaas and Mario Silva on an earlier draft of the paper are deeply appreciated.

References

Al-Abbad, M., Sanni, M., Kokal, S., Krivokapic, A., Dye, C., Dugstad, Ø., Hartvig, S., Huseby, O., 2016. A step-change for Single Well Chemical Tracer Tests SWCTT: field pilot testing of new sets of novel tracers. SPE-181408-MS. In: SPE Annual Technical Conference and Exhibition. Sept, Dubai, UAE, pp. 26–28.

Al-Shalabi, E.W., Luo, H., Delshad, M., Sepehrnoori, K., 2017. Single-well chemical tracer modeling of low salinity water injection in carbonates. SPE. https://doi.org/10.2118/173994-MS.

Aster, R.C., Borchers, B., Thurber, C.H., 2005. Parameter Estimation and Inverse Problems. Elsevier Academic Press, Burlington, p. 301.

Bandura, A.V., Lvov, S.N., 2006. The ionization constant of water over wide ranges of temperature and density. J. Phys. Chem. Ref. Data 35 (1), 15–30.

Bear, J., 1979. Hydraulics of Groundwater. McGraw-Hill, p. 569.

Carlisle, C., Al-Maraghi, E., Al-Saad, B., Britton, C., Fortenberry, R., Pope, G., 2014. One-spot pilot results in the Sabriyah-Mauddud carbonate formation in Kuwait using a novel surfactant emulsion. SPE, 169153.

Chang, M.M., Maerefat, N.L., Tomutsa, L., Honarpour, M.M., 1988. Evaluation and comparison of residual oil determination techniques. SPE Form. Eval. 3 (1), 251–262.

Cockin, A.P., Malcolm, L.T., McGuire, P.L., Giordano, R.M., Sitz, C.D., 2000. Analysis of a Single-Well Chemical Tracer Test to Measure the Residual Oil Saturation to a Hydrocarbon Miscible Gas Flood at Prudhoe Bay. SPE. https://doi.org/10.2118/68051-PA.

Comsol Multiphysics, 2018. User Guide.

Cook, C.E., 1971. Method of determining fluid saturations in reservoirs. US patent No 3, 590–923.

Deans, H.A., 1971. Method of determining fluid saturations in reservoirs. U.S. Patent 3, 623–842.

Deans, H.A., Carlisle, C.T., 1986. Single-well Tracer Tests in Complex Pore Systems. SPE/DOE, 14886.

Deans, H.A., Carlisle, C., 2007. The single-well chemical tracer test – a method for measuring reservoir fluid saturations in situ. Lake, L.W. (Ed.). Petrol. Eng. Handk. 5. Res. Eng. Petrophys., Holstein, E.W. (Ed.), SPE, 615-649.
Deans, H.A., Ghosh, R., 1994. pH and reaction rate changes during single-well chemical tracer tests. SPE. https://doi.org/10.2118/27801-MS.
Deans, H.A., Majoros, S., 1980. The Single-Well Chemical Tracer Method for Measuring Residual Oil Saturation. U.S. Department of energy, p. 119. Final report.
Doorwar, S., Tagavifar, M., Dwarakanath, V., 2020. A 1D Analytical Solution to Determine Residual Oil Saturations from Single-Well Chemical Tracer Test. SPE-200420-MS.
Fortenberry, R., Suniga, O., Delshad, M., Singh, B., Alkaaoud, H.A., Carlisle, C.T., Pope, G.A., 2016. Design and demonstration of new Single-Well Tracer Test for viscous chemical Enhanced-Oil-Recovery fluids. SPE J. 1075–1085. SPE 178914.
Ghosh, R.S., 1994. Effects of pH on Tracer Reaction (Ester Hydrolysis) Rate in Single Well Chemical Tracer Test for Residual Oil Saturation – a Quantitative Approach. Master thesis, University of Wyoming.
Høgnesen, E.J., Strand, S., Austad, T., 2005. Waterflooding of Preferential Oil-Wet Carbonates: Oil Recovery Related to Reservoir Temperature and Brine Composition. SPE 94166.
International Critical Tables, first ed., 1930. Natl. Research Council, McGraw-Hill Book Co. Inc., New York City, VII, pp. 128–141.
Jerauld, G.R., Mohammadi, H., Webb, K.J., 2010. Interpreting single well chemical tracer tests. In: SPE Paper 129724.
Kazemi, N., Korrani, A., Jerauld, G., Al-Qattan, A., 2019. Improved interpretation of single-well-chemical-tracer for low salinity and polymer flooding. SPE.
Khaledialidusti, R., Kleppe, J., Enayatpour, S., 2014. Evaluation and Comparison of Available Tracer Methods for Determining Residual Oil Saturation and Developing an Innovative Single Well Tracer Technique: Dual Salinity Tracer. IPTC-17990-MS.
Khaledialidusti, R., Kleppe, J., Skrettingland, K., 2015. Numerical interpretation of single well chemical tracer (SWCT) tests to determine residual oil saturation in Snorre Reservoir. SPE- 174378-MS. In: EUROPEC 2015. June, Madrid, Spain, pp. 1–4.
Khaledialidusti, R., Kleppe, J., 2017. A comprehensive framework for the theoretical assessment of the single-well-chemical-tracer tests. J. Petrol. Sci. Eng. 159, 164–181.
Khaledialidusti, R., Kleppe, J., 2018. Significance of geochemistry in single-well chemical-tracer tests by coupling a multiphase-flow simulator to the geochemical package. SPE J. 1126–1144.
Mechergui, A., Romero, C., Ganzo, M., 2012. Design of SWTT at high salinity and high temperature: where are the limits? SPE, 155515.
Millington, R.J., Quirk, J.M., 1961. Permeability of Porous Solids. Trans, Faraday.
Park, Y.J., 1989. Thermal Effects of Single-Well Chemical Tracer Tests for Measuring Residual Oil Saturation. PhD Thesis. University of Houston, p. 209.
Park, Y.J., Deans, H.A., Tezduyar, T.E., 1991. Thermal effects on single-well chemical tracer tests for measuring residual oil saturation. SPE Form. Eval. 6, 401–408.
Pedersen, T., 2018. Properly designed temperature history nanoparticles may improve residual oil saturation estimates from SWCT tests. J. Petrol. Sci. Eng. 170, 383–391.
Pedersen, T., 2021. Temperature gradient and pH effects on Sor estimates from SWCT tests - the no buffer case. J. Petrol. Sci. Eng. 196 https://doi.org/10.1016/j.petrol.2020.107652.
Plummer, L.N., Busenberg, E., 1982. The solubilities of calcite, ankerite and vaterite in CO_2-H_2O solutions between 0 and 90 °C, and an evaluation of the aqueous model for the system $CaCO_3$-CO_2-H_2O. Geochem. Cosmochim. Acta 46, 1011–1040.
Ramey Jr., H.J., 1962. Wellbore heat transmission. SPE J. Petrol. Technol. 96, 427–435.
Shook, G.M., Pope, G.A., Asakawa, K., 2009. Determining reservoir properties and flood performance from tracer test analysis. SPE 124614.
Skrettingland, K., Holt, T., Tweheyo, M.T., Skjevrak, I., 2010. Snorre low salinity water injection – core flooding and Single Well field pilot. SPE, 129877.
Teklu, T.W., Brown, J.S., Kazemi, H., Graves, R.M., AlSumati, A.M., 2013. A critical literature review of laboratory and field scale determination of residual oil saturation. In: SPE 164483. SPE Prod. Operat. Symp. March, Oklahoma City, Oklahoma, pp. 23–26.
Tomich, J.F., Dalton Jr., R.L., Deans, H.A., Shallenberger, L.K., 1973. Single-well tracer method to measure residual oil saturation. J. Petrol. Geol. 211–218.
Wellington, S.L., Richardson, E.A., 1994a. A single-well tracer test with in-situ-generated CO_2 as the oil tracer. SPE Reservoir Eng. 85–91.
Wellington, S.L., Richardson, E.A., 1994b. Redesigned ester single-well tracer test that incorporates pH-driven hydrolysis rate changes. SPE Reservoir Eng. 233–239.
Wellington, S.L., Richardson, E.A., 1994c. Simultaneous use of ester and CO_2 single-well tracers. SPE Reservoir Eng. 240–246.